Alloying, elemental enrichment, and interdiffusion during the growth of Ge(Si)/Si(001) quantum dots

X. Z. Liao,[1,2,*] J. Zou,[1] D. J. H. Cockayne,[3] J. Wan,[4] Z. M. Jiang,[4,5] G. Jin,[4] and Kang L. Wang[4]
[1]*Australian Key Center for Microscopy & Microanalysis, The University of Sydney, Sydney NSW 2006, Australia*
[2]*Division of Materials Science and Technology, Los Alamos National Laboratory, Los Alamos, New Mexico 87545*
[3]*Department of Materials, University of Oxford, Parks Road, Oxford OX1 3PH, England*
[4]*Device Research Laboratory, Electrical Engineering Department, University of California at Los Angeles, Los Angeles, California 90095-1594*
[5]*Surface Physics Laboratory, Fudan University, Shanghai 200433, China*
(Received 2 October 2001; published 27 March 2002)

Ge(Si)/Si(001) quantum dots produced by gas-source molecular beam epitaxy at 575 °C were investigated using energy-filtering transmission electron microscopy and x-ray energy dispersive spectrometry. Results show a nonuniform composition distribution in the quantum dots with the highest Ge content at the dot center. The average Ge content in the quantum dots is much higher than in the wetting layer. The quantum dot/substrate interface has been moved to the substrate side. A growth mechanism of the quantum dots is discussed based on the composition distribution and interfacial structures.

DOI: 10.1103/PhysRevB.65.153306 PACS number(s): 68.65.Hb, 68.35.Dv, 68.37.Lp

Since the discovery that coherent (dislocation-free) semiconductor quantum dot (QD) islands can be formed through Stranski-Krastanow (SK) growth, in which a layer-by-layer grown flat wetting layer is followed by island formation in lattice-mismatched heteroepitaxial systems,[1] the SK growth QD islands have attracted considerable attention because of their potential electronic and optoelectronic applications.[2] The composition of QD's has been the subject of intense investigation[3–6] because of its importance in understanding the structure-property relationship of QD's.[7] However, there has been relatively little investigation of the relationship between the nature of QD growth and the composition distribution.[8,9]

Many transmission electron microscopy (TEM) techniques, including spectrum techniques[6,10] and imaging techniques,[3,9,11] have been used for QD local composition investigations. Electron-energy-filtering imaging (EFI) in the analytical TEM is of particular importance for the investigation of heteroepitaxial structures,[9] because it can provide information not only about the elemental distribution at nanometer resolution,[12] but also about the interfacial morphology. In this paper, we report an EFI investigation of the microstructure and chemistry of Ge(Si)/Si(001) QD's and discuss a possible growth mechanism that leads to the observed results.

A Ge/Si(001) sample consisting of ten layers of Ge QD's separated by about 40 nm of Si spacer layers was grown using gas-source molecular beam epitaxy (MBE) with a Si_2H_6 gas source and a Ge effusion cell at a temperature of 575 °C. The Ge deposition thickness at each layer was 1.6 nm with a growth rate of 0.4 nm/min. In this paper, we concentrate only on the top unburied QD islands. Cross-section TEM specimens were prepared using mechanical thinning followed by Ar^+-ion-beam thinning in a Gatan precision ion polishing system (PIPS) with an accelerating energy of 3 keV. A cross-section TEM investigation was carried out using a Philips CM120 operated at 120 kV equipped with a Gatan imaging filter (GIF) system and also using a VG 601B scanning transmission electron microscope operated at 100 kV equipped with an Oxford x-ray energy dispersive spectroscopy (EDX) system. Elemental mapping was performed with the GIF using the three-window technique.[13] The Si $L_{2,3}$ edge at 99.2 eV in the electron energy loss spectrum was used for Si mapping, and the centers of two pre-edge windows were set at 60 and 80 eV with a slit width of 20 eV. Ge maps were obtained using the Ge $L_{2,3}$ edge at 1217 eV with the centers of two pre-edge windows set at 1117 and 1177 eV and a larger slit width of 60 eV to increase the image intensity at higher energy loss so that focusing of the images is possible.

Because the background removal procedure in the three-window technique is unable to totally eliminate the intensity changes caused by diffraction contrast variations that occur between images acquired at different energy losses, leaving artifacts in the final EFI,[14,15] strong diffraction conditions were avoided by orienting the specimen away from any main zone axis, but keeping the QD/substrate interface aligned with the electron beam.

To carry out quantitative elemental distribution investigation using EFI, it is important that the TEM specimen be sufficiently thin for the electrons detected to be dominated by single scattering.[12] For elemental analysis using edges above 1000 eV, the specimen can be relatively thick because multiple scattering can be ignored if $t/\lambda < 2$,[16] where t is the specimen thickness and λ is the mean free path for a plasmon excitation. However, for edges below 1000 eV, t/λ needs to be smaller than 0.5.[17] The specimen thickness can be measured from the electron energy loss spectrum using the relationship $t/\lambda = \ln(I_{total}/I_0)$,[18] where I_{total} is the total spectrum intensity and I_0 is the integrated intensity of the zero-loss peak.

Figure 1(a) shows a typical unfiltered TEM image of an island, i.e. I_{total}. Figure 1(b) shows the same island imaged using zero-loss electrons, i.e. I_0. Figure 1(c) shows I_{total}/I_0, and Fig. 1(d) shows the values of I_{total}/I_0 along the white

 ©2002 The American Physical Society

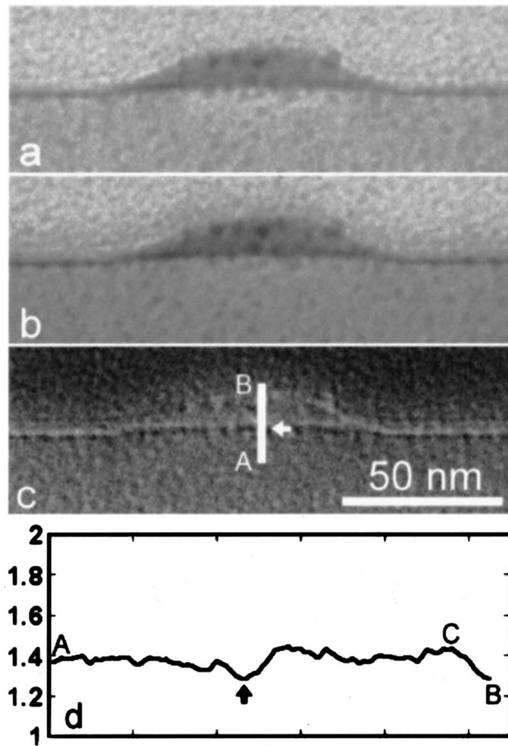

FIG. 1. (a) Unfiltered TEM image of a Ge(Si)/Si(001) QD island giving a total electron intensity I_{total}, (b) filtered TEM image of the same area obtained from zero-loss electron beam providing I_0, (c) result of (I_{total}/I_0) which can be related to specimen thickness at local area, and (d) value of (I_{total}/I_0) along the white line in (c). A white arrow in (c) and a dark arrow in (d) mark the position of the island/substrate interface in the sample.

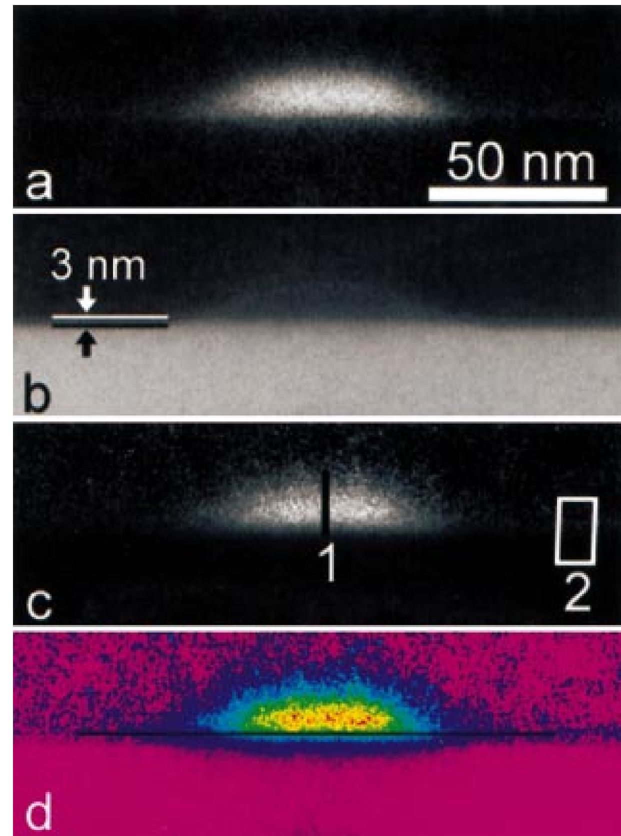

FIG. 2. (Color) (a) Ge elemental map of the island shown in Fig. 1 and (b) Si map of the same island. A dark line and a white line are drawn along the lower and upper boundaries of the semitransparent wetting layer, respectively, to show the layer thickness. (c) Result of the Ge map divided by the Si map. (d) Pseudocolor (spectrum) image showing the intensity (brightness) distribution of (c). A dark line is drawn passing through the wetting layer/substrate interface.

line in Fig. 1(c). From Fig. 1(d) it is clear that (I_{total}/I_0) in the Si substrate [the island/substrate interface is marked with a white arrow and a dark arrow in Figs. 1(c) and 1(d), respectively] is below 1.40 and increases to about 1.46 above the interface because of the change of chemical composition. The value of 1.40 at the substrate gives $t/\lambda<0.34$ in the substrate. Using $\lambda=115$ nm for Si at 100 keV,[19] the substrate thickness $t=39$ nm. In contrast to the relatively smooth intensity curve in the substrate area, (I_{total}/I_0) in the QD island fluctuates, with the highest value of 1.46 near the QD/substrate interface and lowest value of 1.30 at the edge of the QD island, giving $0.26<t/\lambda<0.38$. Two possible reasons may be responsible for the relatively large fluctuation of t/λ: (1) local thickness (t) variations and/or (2) local composition variations that result in the change of λ. Because we are not sure if the local specimen thickness is a constant, a direct comparison of local composition within the island using the intensity of EFI images will be less reliable. To cancel the intensity change in EFI images possibly induced by thickness variations, the atomic ratio map technique[12] is used, in which the atomic ratio of two elements is related to the ratio of their elemental map intensities by a k factor (ratio of partial ionization cross sections of the two elements). However, because the parameters (recording time, beam convergence, slit width, etc.) for acquiring the Ge and Si maps are different, determining a k factor is very difficult. As a result, employing this technique in this investigation provides only a relative composition distribution.

Figure 2(a) is a typical EFI of the island showing a Ge map where the brightness corresponds to the Ge content projected normal to the image. It is clear that the image intensity (brightness) of the island is much higher than that of the wetting layer, which appears as a fuzzy white line, implying a much higher Ge concentration in the island than in the wetting layer. (Note that because of the relatively thick wetting layer [see Fig. 2(b)], the image intensity will not be smeared out by a loss in the image resolution.) Figure 2(b) is a typical Si map of the island. A wetting layer of about 3 nm thickness, as marked between a dark and a white line in Fig. 2(b), with semitransparent contrast above the Si substrate is seen in the Si map. The thickness and contrast seen in the Si map all imply that the wetting layer is a GeSi alloy. Figure 2(c) shows the result of the Ge map in Fig. 2(a) divided by the Si map in Fig. 2(b). The intensity in Fig. 2(c) can be directly related to the local atomic ratio of Ge and Si by a k factor. The intensity profile along the dark line (marked with "1") passing through the island in Fig. 2(c) is plotted in Fig. 3 (also marked with "1"), showing that the highest intensity is located at the middle of the island. The intensity profile

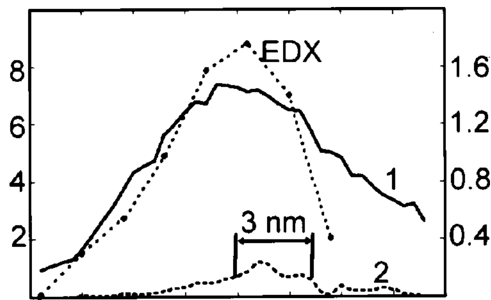

FIG. 3. Intensity profile along the dark line drawn in Fig. 2(c) (I_{Ge}/I_{Si}) and EDX values along the same line. The left coordinate is the EFI intensity ratio, and the right coordinate is the EDX intensity ratio of Ge-*K*/Si-*K*. The intensity profile along the white rectangle area in Fig. 2(c) is also presented, and the wetting layer thickness is obtained from the full width at half maximum of the wetting layer peak.

along the white rectangle (marked with "2") in a wetting layer area in Fig. 2(c) is also plotted in Fig. 3 (marked with "2" also) and the full width at half maximum of the wetting layer peak conforms to a wetting layer thickness of about 3 nm.

To further confirm the results obtained from EFI, an EDX measurement of Ge and Si was carried out along the dark line in Fig. 2(c) and the result of the intensity ratio of the Ge-*K* peak and Si-*K* peak is also presented in Fig. 3, demonstrating a very similar relative composition concentration distribution profile to the results obtained from EFI.

To see more clearly the intensity distribution and the interfacial structure in Fig. 2(c), a pseudocolor (spectrum) image of Fig. 2(c) is shown in Fig. 2(d) where the highest intensity is presented in red color and the lowest intensity in purple. A horizontal dark line is drawn in Fig. 2(d) along the wetting layer/substrate interface. It is seen that Ge has diffused down below the dark line and the area with the highest intensity is above the dark line.

To explain the above experimental phenomena, we note that Tersoff[8] has suggested that when islands nucleate on a strained alloy, segregation of the larger-mismatch component to the islands occurs to reduce the nucleation barrier and, because the optimum composition is the same at any island size, the enrichment of the larger-misfit element to the islands will continue during the island growth. This will result in a compositionally depleted wetting layer if the island growth continues after the incident flux is turned off and will result in progressively reducing the larger-misfit component in the outmost layers of the islands. Tersoff also commented[8] that if the growth is limited by surface diffusion, then since Ge diffuses much more quickly than Si, even greater Ge enrichment will occur. Although in this work nominally pure Ge is deposited on Si(001), it is believed that, from the above experimental evidence and previous reports,[20,21] the forming wetting layer is in fact a GeSi alloy due to the intermixing with the substrate. Ge buildup by segregation on the surface of this initial flat layer is considered the driving force for islanding. However, while the mechanism suggested by Tersoff[8] can explain the observed results, the extent of segregation reported here appears to exceed the values predicted by his work.

The enrichment of Ge in the islands reduces the energetic barrier of islanding. On the other hand, it increases the strain energy between the island and substrate. This strain energy is then reduced by further alloying of the island material with the substrate, and this is evidenced by the interdiffusion of Ge and Si at the island/substrate interface. The interdiffusion results in the island/substrate interface moving down to the substrate side, as seen in Fig. 2(d), and the highest Ge content area in the islands, which is originally located at the initial island/substrate interface, as predicted by Tersoff,[8] moving up to the middle of the islands.

It is not surprising that this composition distribution is different from our previous results on Ge(Si)/Si(001) grown at 700 °C in which (i) the island top has the highest Ge content and the island bottom has the lowest Ge content[10] and (ii) a trench was observed around each island,[22] but is not seen in our current investigation. Chaparro *et al.*[23] also reported similar trenches and similar composition distributions to our previous reports. The explanation for these observations is that high temperatures result in increased elemental interdiffusion at the island/substrate interface as has been evidenced in our previous report,[22] and this results in the high Ge content moving further up the island. The larger elemental activation energies at high temperatures allows an elemental redistribution so that the system can release strain energy as much as possible.

In conclusion, the epitaxial growth of Ge(Si)/Si(001) QD islands involves a complex series of processes including alloying of the deposited material with the substrate material, enrichment of the larger-mismatch element (Ge) into the islands, elemental interdiffusion between the islands and substrate, and elemental redistribution within the islands. Different growth kinetics may result in totally different composition distributions within the islands.

The authors thank the Australian Research Council for financial support. This project is also partially supported by ARO and the Semiconductor Research Corporation.

*Electronic address: xzliao@lanl.gov

[1] D. J. Eaglesham and M. Cerullo, Phys. Rev. Lett. **64**, 1943 (1990).
[2] J. Y. Marzin, J. M. Gerard, A. Izraal, D. Barrier, and G. Bastard, Phys. Rev. Lett. **73**, 716 (1994).
[3] N. Liu, J. Tersoff, O. Baklenov, A. L. Holmes, and C. K. Shih, Phys. Rev. Lett. **84**, 334 (2000).
[4] X. Z. Liao, J. Zou, D. J. H. Cockayne, R. Leon, and C. Lobo, Phys. Rev. Lett. **82**, 5148 (1999).
[5] A. Rosenauer, U. Fisher, D. Gerthsen, and A. Förster, Appl. Phys. Lett. **71**, 3868 (1997).
[6] T. Walther, C. J. Humphreys, and A. G. Cullis, Appl. Phys. Lett. **71**, 809 (1997).
[7] W. D. Sheng and J. P. Leburton, Phys. Rev. B **63**, 161301 (2001).
[8] J. Tersoff, Phys. Rev. Lett. **81**, 3183 (1998).
[9] T. Walther, A. G. Cullis, D. J. Norris, and M. Hopkinson, Phys.

Rev. Lett. **86**, 2381 (2001).

[10] X. Z. Liao, J. Zou, D. J. H. Cockayne, Z. M. Jiang, X. Wang, and R. Leon, Appl. Phys. Lett. **77**, 1304 (2000).

[11] S. Kret, T. Benabbas, C. Delamarre, Y. Androussi, A. Dubon, J. Y. Laval, and A. Lefebvre, J. Appl. Phys. **86**, 1988 (1999).

[12] F. Hofer, W. Grogger, G. Kothleitner, and P. Warbichler, Ultramicroscopy **67**, 83 (1997).

[13] L. Reimer, *Energy-Filtering Transmission Electron Microscopy* (Springer, Berlin, 1995), p. 347.

[14] F. Hofer, P. Warbichler, and W. Grogger, Ultramicroscopy **59**, 15 (1995).

[15] K. T. Moore, J. M. Howe, and D. C. Elbert, Ultramicroscopy **80**, 203 (1999).

[16] R. F. Egerton, Y. Y. Yang, and F. Y. Y. Chen, Ultramicroscopy **38**, 349 (1991).

[17] P. A. Crozier, Ultramicroscopy **58**, 157 (1995).

[18] J. J. Hren, J. I. Goldstein, and D. C. Joy, *Introduction to Analytical Electron Microscopy* (Plenum, New York, 1979), p. 278.

[19] T. Malis, S. C. Cheng, and R. F. Egerton, J. Electron Microsc. Tech. **8**, 193 (1988).

[20] B. A. Joyce, J. L. Sudijono, J. G. Belk, H. Yamaguchi, X. M. Zhang, H. T. Dobbs, A. Zangwill, D. D. Vvdensky, and T. S. Jones, Jpn. J. Appl. Phys., Part 1 **36**, 4111 (1997).

[21] M. Krishnamurthy, A. Lorke, M. Wassermeier, D. R. M. Williams, and P. M. Petroff, J. Vac. Sci. Technol. B **11**, 1384 (1993).

[22] X. Z. Liao, J. Zou, D. J. H. Cockayne, J. Qin, Z. M. Jiang, X. Wang, and R. Leon, Phys. Rev. B **60**, 15 605 (1999).

[23] S. A. Chaparro, J. Drucker, Y. Zhang, D. Chandrasekhar, M. R. McCartney, and D. J. Smith, Phys. Rev. Lett. **83**, 1199 (1999).